ORIGINAL ARTICLE

Proteaceae from phosphorus-impoverished habitats preferentially allocate phosphorus to photosynthetic cells: An adaptation improving phosphorus-use efficiency

Patrick E. Hayes[1,2] | Peta L. Clode[2,1] | Rafael S. Oliveira[3,1] | Hans Lambers[1]

[1]School of Biological Sciences, The University of Western Australia, Perth, Western Australia 6009, Australia

[2]Centre for Microscopy, Characterisation and Analysis, The University of Western Australia, Perth, Western Australia 6009, Australia

[3]Departamento de Biologia Vegetal, Universidade Estadual de Campinas, Campinas 13083-862, Brazil

Correspondence
Patrick E. Hayes, School of Biological Sciences, The University of Western Australia, 35 Stirling Highway, Perth, Western Australia 6009, Australia.
Email: patrick.hayes@research.uwa.edu.au

Funding information
Coordenação de Aperfeiçoamento de Pessoal de Nível Superior, Grant/Award Number: 88881.068071/2014-01; Australian Research Council, Grant/Award Number: DP130100005

Abstract

Plants allocate nutrients to specific leaf cell types; eudicots are thought to predominantly allocate phosphorus (P) to epidermal/bundle sheath cells. However, three Proteaceae species have been shown to preferentially allocate P to mesophyll cells instead. These Proteaceae species are highly adapted to P-impoverished habitats, with exceptionally high photosynthetic P-use efficiencies (PPUE). We hypothesized that preferential allocation of P to photosynthetic mesophyll cells is an important trait in species adapted to extremely P-impoverished habitats, contributing to their high PPUE. We used elemental X-ray mapping to determine leaf cell-specific nutrient concentrations for 12 Proteaceae species, from habitats of strongly contrasting soil P concentrations, in Australia, Brazil, and Chile. We found that only species from extremely P-impoverished habitats preferentially allocated P to photosynthetic mesophyll cells, suggesting it has evolved as an adaptation to their extremely P-impoverished habitat and that it is not a family-wide trait. Our results highlight the possible role of soil P in driving the evolution of ecologically relevant nutrient allocation patterns and that these patterns cannot be generalized across families. Furthermore, preferential allocation of P to photosynthetic cells may provide new and exciting strategies to improve PPUE in crop species.

KEYWORDS

calcium accumulation, cell-type-specific distribution, elemental analysis, scanning electron microscopy, X-ray microanalysis

1 | INTRODUCTION

Plants often acquire nutrients in excess of immediate demands and store them until required. This process of acquisition and storage must be tightly regulated, as particular elements can negatively interact with each other. For example, phosphorus (P) and calcium (Ca) must be stored separately to avoid the precipitation of calcium phosphate, which reduces the availability of both nutrients and severely impacts cellular processes (Conn & Gilliham, 2010; White & Broadley, 2003). Phosphorus is stored in leaves, as it is vital to many processes, such as carbon metabolism, energy transfer, and growth. However, leaves also accumulate Ca, which is transported via transpiration, from root to shoot, where it is accumulated in leaf cell vacuoles and is involved in cell structure and signalling (Gilliham et al., 2011; White, 2001). Therefore, both P and Ca are accumulated in plant leaves, where their separation must be maintained to avoid the deleterious precipitation of

calcium phosphate (Conn & Gilliham, 2010; White & Broadley, 2003). We still know very little about the patterns and processes of cell-specific nutrient allocation despite its obvious importance to overall plant nutrition and physiology.

The current model of cell-specific nutrient allocation is based on a recent review by Conn and Gilliham (2010) and suggests that eudicots generally allocate P to epidermis (EP) and bundle sheath (BS) cells and Ca to mesophyll cells. However, in contrast to this model, it has been shown that some species of Proteaceae from severely P-impoverished habitats in south-western Australia (Lambers, Finnegan, et al., 2015; Shane, McCully, & Lambers, 2004) and South Africa (Hawkins, Hettasch, Mesjasz-Przybylowicz, Przybylowicz, & Cramer, 2008) preferentially allocate P to mesophyll cells and not to EP or BS cells.

The family Proteaceae are mainly found across the southern hemisphere and are most abundant in severely P-impoverished habitats, for example, south-western Australia (>680 sp.) and South Africa (>330

sp.; Weston, 2007; Sauquet et al., 2009; Lambers, Clode, et al., 2015), with much lower abundances in regions of higher P-fertility, for example, Chile (7 sp.) and Brazil (33 sp.; Pate, Verboom, & Galloway, 2001; Sauquet et al., 2009). Proteaceae species that are abundant in P-impoverished habitats represent a major component of the vegetation and have key roles in ecosystem functioning (Cowling & Lamont, 1998; Lambers et al., 2012). To be abundant in such severely P-limited habitats, these Proteaceae species must use the low amounts of available P far more efficiently, and this is reflected in their exceptionally high rates of photosynthetic P-use efficiency (PPUE; Table S1; Wright et al., 2004; Denton, Veneklaas, Freimoser, & Lambers, 2007; Lambers, Bishop, Hopper, Laliberté, & Zúñiga-Feest, 2012; Lambers, Clode et al., 2015; Lambers, Finnegan et al., 2015). These exceptionally high PPUE values are achieved through a combination of adaptations, including replacement of phospholipids by sulfolipids and galactolipids (Lambers et al., 2012) and functioning at very low levels of ribosomal RNA (Sulpice et al., 2014). In addition, we surmise that the ability of some Proteaceae to preferentially allocate P to photosynthetic mesophyll cells (where P is needed in the greatest amount), unlike other eudicots, may contribute to these species' exceptionally high PPUE (Lambers, Finnegan, et al., 2015; Stitt, Lunn, & Usadel, 2010; Tsujii, Oikawa, & Kitayama, 2017). However, this leads us to the question, is this is a family-wide trait? That is, do Proteaceae from relatively P-rich habitats also show a preferential allocation of P to mesophyll cells, or has this only evolved in species from severely P-impoverished habitats? Furthermore, does Ca allocation reflect the current model, or does this also differ?

To address the above questions, we used quantitative X-ray elemental analysis to determine leaf cell-specific nutrient concentrations and distributions for a phylogenetically disperse range of 12 Proteaceae species, from three habitats of contrasting soil [P], in Australia, Brazil, and Chile (Weston & Barker, 2006). These habitats represent an extreme range in total soil [P], from the extremely P-impoverished south-western Australia (Denton et al., 2007; Lambers, Brundrett, Raven, & Hopper, 2010) to the relatively P-rich soils of South America: Brazil (Lannes, Bustamante, Edwards, & Olde, 2016; Miatto, Wright, & Batalha, 2016) and Chile (Borie & Rubio, 2003; Delgado, Zúñiga-Feest, Almonacid, Lambers, & Borie, 2015). Species from south-western Australia are highly adapted to their severely P-impoverished habitat, showing low whole leaf [P] compared with South American species (Lambers et al., 2010) and much higher PPUE (Table S1; Wright et al., 2004; Denton et al., 2007; Lambers et al., 2012).

Many studies have assessed cell-specific nutrients in leaves of metal-hyperaccumulating and crop species, from which the current model (Conn & Gilliham, 2010) is largely based (Ager, Ynsa, Domínguez-Solís, Gotor, et al., 2002; Ager, Ynsa, Domínguez-Solís, López-Martín, et al., 2003; Bidwell, Crawford, Woodrow, Sommer-Knudsen, & Marshall, 2004; Fernando, et al., 2006; Fernando et al., 2008; Küpper, Zhao, & McGrath, 1999; Küpper, Lombi, Zhao, & McGrath, 2000; Küpper, Lombi, Zhao, Wieshammer, & McGrath, 2001; Mesjasz-Prybylowicz & Pineda, 2001; Mesjasz-Przybyłowicz, Balkwill, Przybyłowicz, & Annegarn, 1994; Mesjasz-Przybylowicz, Przybylowicz, Rama, & Pineda, 2001; Regvar et al., 2013; Rios et al., 2012; Treeby, van Steveninck, & de Vries, 1987; Villafort Carvalho et al., 2015; Vogel-Mikuš et al., 2008; Vogel-Mikuš, Pongrac, & Pelicon,

2014; Zhao, Lombi, Breedon, & McGrath, 2000). However, few studies have quantitatively assessed cellular [P], and no study has yet assessed it across a wide range of naturally occurring species, covering an extreme range in soil [P]. This is important, because species occurring in natural habitats with low concentrations of heavy metals are likely very different from metal-hyperaccumulating and crop species. Furthermore, although some studies have assessed individual Proteaceae, this study, for the first time, has investigated patterns of cell-specific nutrient allocation across the broader Proteaceae family, including species from extremely P-impoverished south-western Australian habitats to the P-rich temperate rainforests of southern Chile. This knowledge will provide valuable insights into how native species have evolved to survive under P-impoverished conditions, with important lessons for future crop breeding to improve nutrient-use efficiency and, more fundamentally, will improve our understanding of the factors influencing cell-specific nutrient allocation in plants.

We hypothesized that P would be preferentially allocated to photosynthetic cells in species from south-western Australia, as an adaptation to their extremely P-impoverished habitat (Lambers, Clode, et al., 2015; Tsujii et al., 2017). We also hypothesized that this is not a family-wide trait, with South American species from P-richer habitats expected to show no preferential allocation of P to photosynthetic cells, as they have not had the same evolutionary pressures to increase their P-use efficiency. We also hypothesized that Ca would accumulate in specific cell types, separate from P, and primarily along the transpiration pathway, because [Ca] must be tightly regulated within plant cells, separated from P to avoid precipitation, and is thought to move through leaves via transpiration (Conn & Gilliham, 2010; Gilliham et al., 2011; White & Broadley, 2003). Overall, this study aimed to provide a comprehensive assessment of cell-specific P and Ca allocation patterns in species adapted to habitats of strongly contrasting soil [P].

2 | MATERIALS AND METHODS

2.1 | Study areas and species selection

The three study areas (Australia, Brazil, and Chile) were selected because Proteaceae species are present at all sites and because they cover a wide range in soil [P] (11 to 1,924 mg total P kg^{-1}; see Table 1 for full soil details). The study area in Australia was located in Jurien Bay, south-western Australia, approximately 200 km north of Perth. The soils in this area were extremely P-impoverished, with soil [P] of 11 mg total P kg^{-1}. Three sites were identified in this study area: two on the ~2-million-year-old Bassendean stage of the Jurien Bay dune chronosequence and one on the much older Peron slopes (Hayes, Turner, Lambers, & Laliberté, 2014; Turner, Hayes, & Laliberté, 2017; Turner & Laliberté, 2015). All samples were collected within <100 m, at each site. The three sites were located within a 9 × 4 km area and were dominated by kwongkan bushland (a Proteaceae-rich shrubland). The study area in Brazil was located in Serra do Cipó, south-eastern Brazil, approximately 80 km north-east of Belo Horizonte. This area was intermediate in terms of total soil [P], with soil [P] of 133 mg total P kg^{-1}, placing it between that of sites in Australia and Chile. All samples were taken from a single site (<100 m). The area was dominated by cerrado vegetation. The study area in Chile was

TABLE 1 Key soil chemical properties and vegetation types of the three study areas

Study area	Vegetation type	Total P (mg kg^{-1})	Olsen P (mg kg^{-1})	Total N (g kg^{-1})	Exchangeable Ca (mg kg^{-1})	CEC (cmol$_c$ kg^{-1})	pH (H$_2$O)
Australia	Kwongkan	11 ± 0.5	0.18 ± 0.02	0.10 ± 0.00	183 ± 27	1.22 ± 0.17	6.1 ± 0.1
Brazil	Cerrado	133 ± 13	2.08 ± 0.03	1.8 ± 0.01	621 ± 208	3.48 ± 0.87	5.4 ± 0.3
Chile	Temperate rainforest	1,924 ± 85	0.69 ± 0.18	7.6 ± 0.06	69 ± 18	1.32 ± 0.12	4.6 ± 0.1

Australia (Jurien Bay, south-western Australia), Brazil (Serra do Cipó, south-eastern Brazil), and Chile (Puerto Montt, southern Chile). Olsen P, a measure of plant-available P. All values are mean ± standard error (n = 3–12).

CEC = cation exchange capacity.

located in Parque Katalapi, Puerto Montt, southern Chile, approximately 1,000 km south of Santiago. All samples were taken from a single site (<100 m). The area had very P-rich young soil and was dominated by temperate rainforest, with soil [P] of 1,924 mg total P kg^{-1}. All sites consisted of soils with low pH (6.1, 5.4, and 4.6, Australia, Brazil and Chile, respectively). The main difference between sites was a clear and strong gradient in total soil [P], which, given the ability of these species to produce P-mining cluster roots, is a good indicator of plant-available P for these species.

Twelve Proteaceae from eight genera were selected. These species were chosen as they are each locally abundant, and, together, they effectively covered a broad range of the Proteaceae phylogeny (Table S2; Weston, 2014). Each study area contained a different set of species. In Australia, seven species were selected, from four genera: *Banksia* (*Banksia attenuata* R.Br., *Banksia menziesii* R.Br., and *Banksia prionotes* Lindl.), *Hakea* (*Hakea incrassata* R.Br. and *Hakea prostrata* R. Br.), *Persoonia* (*Persoonia comata* Meisn.), and *Petrophile* (*Petrophile macrostachya* R.Br.). A single species was selected from Brazil from the genus *Roupala* (*Roupala montana* Aubl.). In Chile, four species were selected, from three genera: *Embothrium* (*Embothrium coccineum* J.R. Forst. & G. Forst.), *Gevuina* (*Gevuina avellana* Mol.), and *Lomatia* (*Lomatia ferruginea* (Cav.) R.Br and *Lomatia hirsuta* (Lam.) Diels ex Macbr.). Species from the same study area were not always closely related. For example, *Lomatia* and *Embothrium* from Chile are more closely related to *Hakea* species from Australia than to other South American species (Weston, 2014). Two to three species were chosen for each of the *Banksia*, *Hakea*, and *Lomatia* genera, allowing for investigation of within-genus variation.

2.2 | Leaf sampling and nutrient analyses

Leaf samples were collected in January (Chile) and November (Australia, Brazil) 2014. Three healthy mature individuals were selected for each species in each study area. From each individual plant, only mature, undamaged, fully expanded, and sun-exposed leaves were sampled. A total of 36 samples were collected for whole-leaf nutrient analyses. All leaf material collected in Australia and Chile was immediately frozen in liquid nitrogen (N), before being freeze-dried and ground using a ball-mill grinder. Material from Brazil was collected and oven dried at 60 °C, for 72 hr, before being ground using a ball-mill grinder. All samples were then acid-digested using concentrated HNO$_3$:HClO$_4$ (3:1), and the concentration of P determined colourimetrically using malachite green method (Motomizu, Wakimoto, & Toei, 1983). In all digests from Australia and Chile, the concentration of Ca was determined by inductively coupled plasma optical emission spectrometry (ChemCentre, Perth, WA, Australia). In all acid digests from Brazil, the concentration of Ca was determined by atomic absorption

spectrometry (Laboratório de Tecidos Vegetais, Escola Superior de Agricultura Luiz de Queiroz, ESALQ-USP, Sao Paulo, Brazil).

2.3 | Soil sampling and analyses

Soil samples were collected in January (Chile), June (Australia), and November (Brazil) 2015.

Samples were taken at 0–20 cm depth, after removal of the litter layer. Nine soil samples were collected in Australia; three representative samples from each of the three sites in Jurien Bay, Australia. Soil samples from Brazil (three) and Chile (12) were collected within 1 m of each individual plant. The soils in Brazil and Chile were collected from each individual because soil properties at these sites are less well known than those in Jurien Bay (Hayes et al., 2014; Turner & Laliberté, 2015), and we aimed for an accurate estimate of soil properties at all sites. There was later found to be no significant difference (p > .05) among sites (Australia) or species (Brazil and Chile) within each study area, and, therefore, all soil properties were simply reported by study area (Australia, Brazil, or Chile).

All samples were sieved (<2 mm) to remove any large organic debris, before being homogenized and air-dried prior to chemical analyses. Samples from Australia and Brazil were analysed at the Smithsonian Tropical Research Institute (Panamá, Repúblic de Panamá). Samples from Chile were analysed at the Laboratorio de Analisis de Suelos y Plantas, Universidad de Concepcion (UdeC, Chillán, Chile) and at the Laboratorio Agricola (Ñuñoa, Santiago, Chile). Total soil [P] was measured by ignition and acid digestion. Olsen P (soil P availability) was measured by sodium bicarbonate extraction and molybdate colourimetry. Total N was measured by dry combustion (Australia and Brazil) and by Kjeldahl digestion with sulphuric and salicylic acid, followed by colourimetric analysis (Chile). In samples from Australia and Brazil, the exchangeable Ca and other cations were determined by BaCl$_2$ (0.1 M) extraction and inductively coupled plasma optical emission spectrometry. In samples from Chile, the exchangeable Ca and other cations were determined using an ammonium acetate (1 M) extraction and atomic absorption spectrometry. Both types of cation extractions (BaCl$_2$ and ammonium acetate) yield similar results for exchangeable cations (Carter & Gregorich, 2008). Soil pH was determined in a 1:2 soil-to-solution ratio in water using a glass electrode.

2.4 | Leaf sampling for cell-specific element analysis and leaf anatomy

Leaf samples for cell-specific element analysis were collected from the same plants and at the same time as for leaf nutrient analysis, in January (Chile) and November (Australia, Brazil) 2014. From each

individual plant, only mature, undamaged, fully expanded, and sun-exposed leaves were sampled. Three to six samples were collected from one to two leaves, for each of the 36 individual plants. Upon removal of a leaf, small sections (~2 × 3 mm) were consistently cut from either side of the mid-rib, mid-way along the leaf, avoiding any large secondary veins. These sections were then mounted onto aluminium pins using optimal cutting temperature compound and plunged into liquid N (Figure S1a), thereby immediately immobilizing and preserving cellular ions. Samples were then stored in liquid N until preparation in a cryomicrotome and analysis using cryo-scanning electron microscopy. With this, all samples were collected fresh in the field, were immediately plunge frozen in liquid N, and were always kept under cryo-conditions, such that all elements were preserved in situ.

Small (~5 × 5 mm) leaf sections of the same plant leaves were also collected for anatomical imaging. These samples were immediately immersed in fixative, composed of 2.5% (vol/vol) glutaraldehyde +1.6% (vol/vol) paraformaldehyde in 10 mM phosphate-buffered saline and left for 24 hr, before being stored at 4 °C. Fixed leaves were then vibratomed to produce transverse leaf sections of ~30–60 μm. These were then mounted in water on glass slides and imaged using bright-field and fluorescence (ultraviolet excitation) illumination on an Axioskop optical microscope (Zeiss, Oberkochen, Germany) fitted with an Axiocam digital camera (Zeiss).

2.5 | Cell-specific element analysis by X-ray microanalytical mapping

Transverse regions of frozen hydrated leaf samples were prepared by cryoplaning a flat surface with a glass knife, followed by a diamond knife, at −120 °C in a cryomicrotome (Leica EM FC6 cryochamber integrated with Leica Ultracut EM UC6 microtome). Leaves were progressively microtomed flat, initially on a glass knife at 1 μm, 750 nm, and 500 nm steps and then finally with fine precision on a diamond knife at 250 and 100 nm steps. The pin was then mounted on a custom-made substage, transferred under an N gas environment to a Leica MED020 cryopreparation system, and sputter coated with 25–50 nm chromium, without sublimation. After coating, samples were transferred under vacuum to a Zeiss field emission scanning electron microscope fitted with a Leica VCT100 cryotransfer and stage, and an Oxford X-Max80 SDD X-ray detector interfaced to Oxford Instruments AZtecEnergy software (Figure S1b). This preparation method and this fully integrated Oxford analytical system have been shown to be highly suitable for elemental analysis and quantitation of biological samples (Huang, Canny, Oates, & McCully, 1994; Jin et al., 2017; Marshall, 2017; Marshall & Clode, 2009; Marshall, Goodyear, & Crewther, 2012; Marshall & Xu, 1998; McCully, Canny, Huang, Miller, & Brink, 2010).

Samples were analysed at −150 °C, 15 kV, and a 2 nA beam current (measured using a faraday cup), in high-current mode. Prior to each map acquisition, the instrument was calibrated, and the beam current was measured using a pure copper standard. Elemental maps were acquired at a resolution of 512 pixels, for >3,000 frames with a dwell time of 10 μs per pixel. Drift correction and pulse-pile up correction were activated. Using the Oxford Instruments AZtecEnergy software, quantitative numerical data were subsequently extracted from regions of interest drawn on the element maps (Figure S1c), with individual

spectra from each pixel within the region of interest summed and processed to yield element concentration data. Summed spectra from regions of interest were quantified using the AZtec XPP model for matrix corrections using standard files included within the software package. Regions of interest represented various areas and individual cells of interest. Different cells were readily identified and classified, based on their leaf anatomy, cell appearance, and element levels. Only cells that were clearly identifiable and had a flat surface were analysed, with airspaces, for example, avoided (Figure S1d,e). Because the central vacuole occupies most of the volume in a plant cell, it is assumed that the reported measurements typically reflect vacuolar concentrations. Different species possess different anatomy and combinations of cell types (Table S3; Figures S2–S6). Overall, the following six cell types were confidently identified and analysed: epidermis (EP), hypodermis (HY), palisade mesophyll (PM), spongy mesophyll (SM), internal parenchyma (IP), and sclerenchyma (SC). In some species, some of these cell types accumulated Ca differentially, with Ca not in all cells. In such cases, these were further subdivided, on the basis of their [Ca]. Calcium-accumulating cells were identified with the suffix "Ca": for example, HY.Ca, PM.Ca, SM.Ca, and IP.Ca. In total, 2,789 cells were analysed, with 7–117 cells analysed for each cell type within each species, across three individual plants (Table S3). The element maps for P are not presented because they did not pictorially reveal the distribution/variations in P, due to the consistently low levels of P; however, quantitation of [P] from regions of interest was still readily achievable (Figure S1f–h).

Use of this method yielded significant advantages. By plunge-freezing samples direct in liquid N, we could prepare samples in the field, avoid loss or movement of elements, and analyse samples in a frozen fully hydrated state, thus measuring cellular concentrations exactly as they were in the field. This has significant advantages over alternative methods, where samples are freeze-dried or freeze-substituted, potentially affecting cell nutrient contents. This method is also appropriate for large-scale experiments, where samples can be stored (in liquid N) and analysed over longer periods. These X-ray microanalytical data are also quantifiable, making the direct comparison of studies possible, including, for the first time, the direct comparison of a range of species in a single family from contrasting habitats. A limitation of this method is that it involves bulk samples, which means the analytical resolution is ~2 μm (sufficient for the analysis of individual plant cells; Marshall, 1982), and the detection limit is a few mmol (Roomans & Dragomir, 2007). There was no freezing damage observed in any samples at the scale of these analyses. On occasion, surface frost was observed in some samples, particularly along the cuticle. This was unavoidable and occurs during transfer of the sample from the microtome to the preparation system, which is technically challenging. These areas were not analysed, and thus, this had no impact on our resulting data. As such, our method of sample preparation is simple, suitable for the field, and the subsequent X-ray microanalysis allows for quantifiable analysis of a range of biologically relevant elements in fully hydrated cells.

2.6 | Statistics

Differences in [P] across cell types, between Australia and South America, were tested using general linear mixed-effect models, with

species and individual plants as the random effects (Pinheiro & Bates, 2000). Differences in nutrient concentrations across cell types, at the species level were tested using general linear mixed-effect models, with individual plants as the random effect (Pinheiro & Bates, 2000). The residuals of each model were visually inspected for heteroscedasticity. In the presence of heteroscedasticity, appropriate variance structures were specified if they significantly improved the model, based on likelihood ratio tests (Pinheiro & Bates, 2000). Data and statistical analyses were performed using the R software platform (R Core Team, 2016) and the nlme package (Pinheiro, Bates, DebRoy, Sarkar, & Core Team, 2016). The effects package (Fox, 2003) was used to determine means and 95% confidence intervals, later used to define the differences among cell types and between Australia and South America.

3 | RESULTS

3.1 | Phosphorus

Species from severely P-impoverished habitats of south-western Australia preferentially allocated P to their photosynthetic mesophyll cells (Figure 1a). These mesophyll cells (PM and SM) showed up to 6.5-fold greater [P] than non-photosynthetic cell types (EP, HY, IP, and SC). The mean cell [P] in Australian species ranged from 1.9 μmol g^{-1} in SC to 12.6 μmol g^{-1} in PM (Figure 1a). In contrast, South American species from relatively P-rich soils did not show a preferential allocation of P to photosynthetic cells. They instead showed similar and consistently low [P] across all cell types, ranging from 2.4 μmol g^{-1} in the HY to 5.1 μmol g^{-1} in the PM (Figure 1a). Hence, preferential allocation of P to photosynthetic mesophyll cells is not a Proteaceae family trait

but appears restricted to those Proteaceae species from severely P-impoverished habitats.

When comparing directly between Australian and South American species, the PM and SM cells of Australian species exhibited 2.5- and 1.7-fold greater mean [P], respectively, compared with that of the South American species (Figure 1b). The EP [P] was very low and showed no significant difference between Australian and South American species (Figure 1b).

At the species level, the highest [P] was 17.2 μmol g^{-1} (PM, *B. attenuata*, Australia; Figure 2). Australian species all showed a clear allocation of P to photosynthetic PM and SM cells, with every species showing the highest [P] in PM, followed by SM (Figure 2). All other cell types in Australian species (EP, HY, IP, and SC) showed low [P] (<5 μmol g^{-1}; Figure 2). Collectively, all Australian species preferentially allocated P to PM and SM.

Two of the South American species (*G. avellana* and *L. hirsuta*) did not show a significant difference in [P] among cell types (Figure 3). *E. coccineum* and *L. ferruginea* showed greater [P] in one photosynthetic cell type (SM), but it was only significantly greater than that in EP in *E. coccineum* and EP/PM.Ca in *L. ferruginea*. *R. montana* showed a greater [P] in both EP and PM but only when compared with that in HY and SM.Ca. Therefore, although there were some differences in [P] among cell types of South American species, none showed a preferential allocation of P to all photosynthetic cells (Figure 3).

On average, whole leaf [P] in Proteaceae species from south-western Australia (0.33 mg g^{-1} DW) was approximately half that of species from South America (0.76 mg g^{-1} DW; Brazil and Chile; Figure 4 and Table S4). Leaf [P] in Proteacea species from south-western Australia ranged from 0.29 mg g^{-1} DW in *P. comata* to 0.4 mg g^{-1} DW in *B. prionotes* (Figure 4 and Table S4). Whereas in South
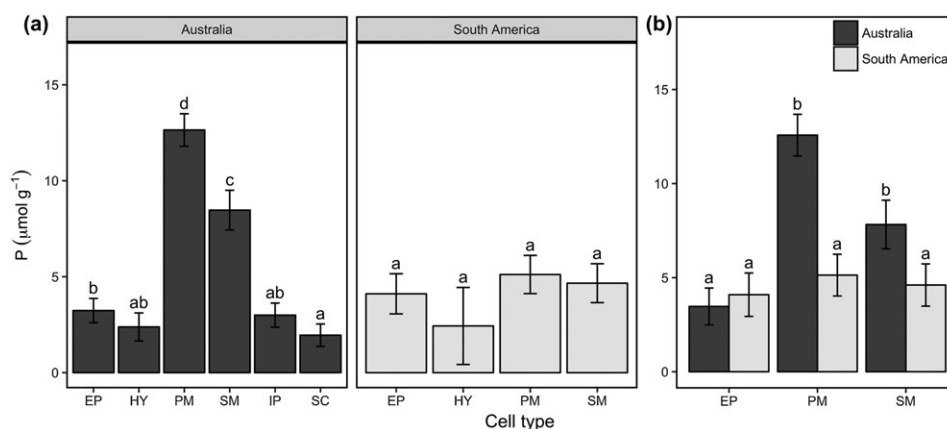

FIGURE 1 Leaf cell-specific phosphorus concentrations ([P]); comparing Proteaceae from P-impoverished habitats in Australia with those from P-rich habitats in South America. (a) Mean cell-specific [P] of Australian and South American species, illustrating differences among cell types within each region. Different sets of cell types are shown, because of differences in leaf anatomy. (b) Mean cell [P] of the common cell types between Australian and South American species, illustrating differences between regions. Common cell types are those found across three or more species in both regions. The hypodermis (HY) is not shown, because it is only found in one South American species. (a–b) This analysis includes all cells within each cell type, because [P] are not significantly different between Ca-accumulating and non-Ca-accumulating cells, of the same cell type. Error bars show 95% confidence intervals from linear mixed-effect models. The different letters indicate significant differences (based on 95% confidence intervals) among cell types (a), or between regions (b). EP = epidermis; IP = internal parenchyma; PM = palisade mesophyll; SC = sclerenchyma; SM = spongy mesophyll
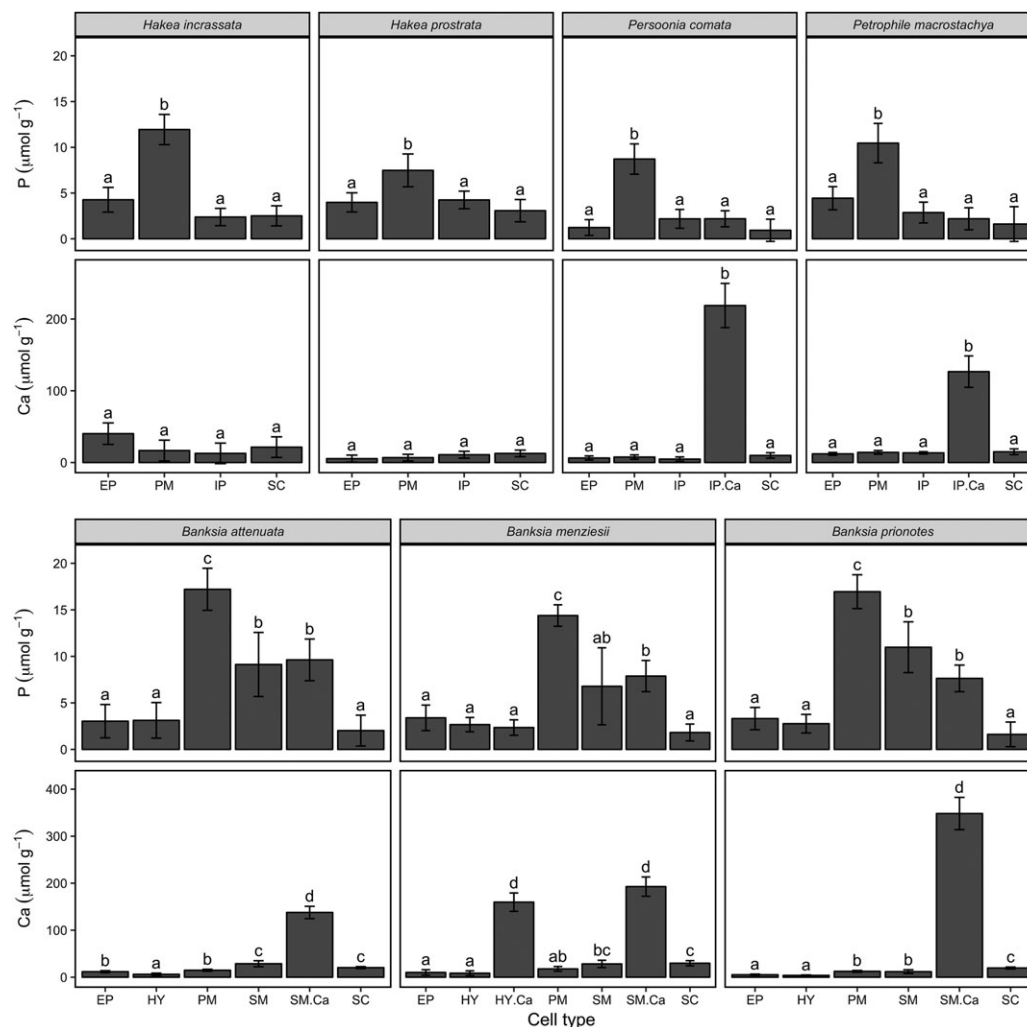
FIGURE 2 Mean leaf cell-specific phosphorus ([P]) and calcium ([Ca]) concentrations across seven Proteaceae species collected from severely P-impoverished soils in south-western Australia. There are different cell types for each species because of differences in anatomy. Concentrations are per unit fresh weight, from fully hydrated cells. Error bars show 95% confidence intervals from linear mixed-effect models. Within each panel, the different letters indicate significant differences among cell types, based on 95% confidence intervals. We did not present element maps for P, because they do not clearly show the distribution of P; however, P was accurately quantified from regions of interest (see Figure S1f–h). EP = epidermis; HY = hypodermis; HY.Ca = hypodermis accumulating Ca; IP = internal parenchyma; IP.Ca = internal parenchyma accumulating Ca; PM = palisade mesophyll; SC = sclerenchyma; SM = spongy mesophyll; SM.Ca = spongy mesophyll accumulating Ca

America, leaf [P] ranged from 0.42 mg g^{-1} DW in *R. montana* (Brazil) to 1.02 mg g^{-1} DW in *E. coccineum* (Chile; Figure 4 and Table S4).

3.2 | Calcium

Calcium was accumulated within specific cells, generally separate from P-accumulating cells (except in *Banksias*) and was not always along the transpiration pathway. There was significant variation in the patterns of Ca accumulation among species, with no distinct shift between species that do and do not allocate P to mesophyll cells (Figures 5–7). In most species, Ca accumulated in IP or SM, with some species also accumulating Ca in other cell types and/or regions (Figures 5–7). *P. comata* and *P. macrostachya* showed Ca accumulation in specific cells of the IP (Figure 5). The *Banksia* and South American species all accumulated Ca in SM (Figures 6 and 7). Furthermore, South American species tended to accumulate Ca in SM cells close to veins, for example, *G. avellana* (Figure 7). *H. prostrata* and *H. incrassata* both accumulated

Ca apoplastically around IP cells but did not significantly accumulate Ca in any specific cell types (Figure 5). *P. comata*, *P. macrostachya*, and all South American species, except *R. montana*, also accumulated Ca apoplastically around adaxial EP cells (Figures 5 and 7). *L. ferruginea* and *L. hirsuta* accumulated Ca in PM as well as SM (Figure 7).

Both *Lomatia* species showed a unique pattern of Ca accumulation, in discrete alternating layers of PM. For example, the uppermost PM layer showed almost no Ca, whereas the second PM layer, immediately beneath it, showed accumulation of Ca up to an exceptionally high 1,413 µmol g^{-1} in *L. ferruginea* (Figures 3 and 7). When four layers of PM were present, the layers of PM from adaxial showed low Ca, high Ca, low Ca, and high Ca. In summary, all species showed evidence of a tight regulation of Ca, allocating Ca within specific cells and/or regions; these were generally within the IP or SM and often associated with veins. Furthermore, only *L. ferruginea* and *L. hirsuta* showed accumulation of Ca in the PM, with a peculiar accumulation of Ca in alternating layers, not previously observed in any plant species.
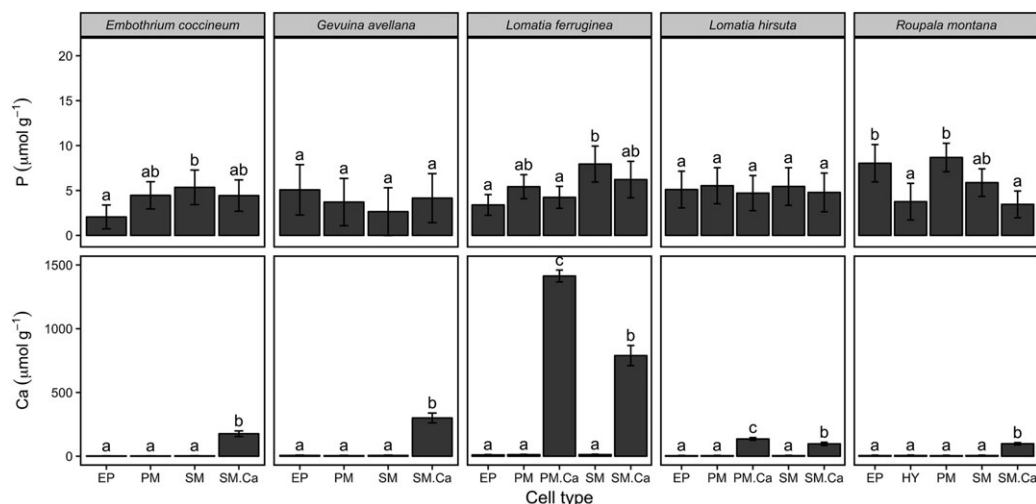
FIGURE 3 Mean leaf cell-specific phosphorus ([P]) and calcium ([Ca]) concentrations across five Proteaceae species collected from relatively P-rich soils in South America. Most species were collected from Puerto Montt in southern Chile, except *Roupala montana*, which was collected in Serra do Cipó, south-eastern Brazil. There are different cell types for each species because of differences in their anatomy. Concentrations are per unit fresh weight, from fully hydrated cells. Error bars show 95% confidence intervals from linear mixed-effect models. Within each panel, the different letters indicate significant differences among cell types, based on 95% confidence intervals. We did not present element maps for P, because they do not clearly show the distribution of P; however, P was accurately quantified from regions of interest (see Figure S1f–h). EP = epidermis; HY = hypodermis; PM = palisade mesophyll; PM.Ca = palisade mesophyll accumulating Ca; SM = spongy mesophyll; SM.Ca = spongy mesophyll accumulating Ca
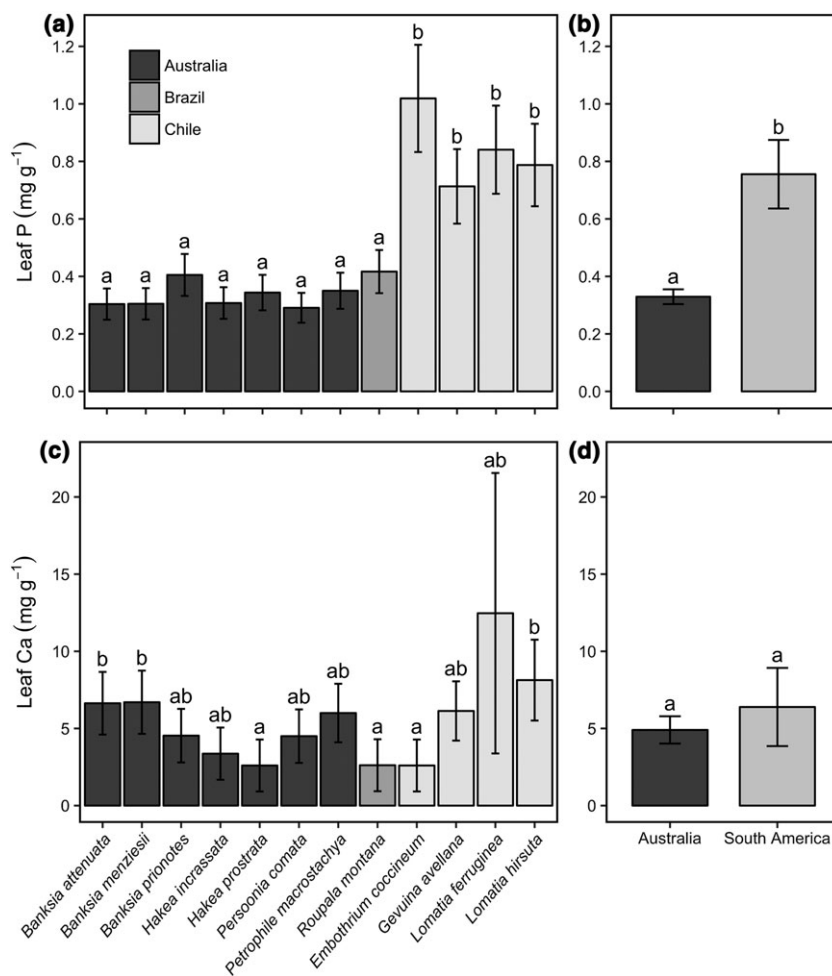

FIGURE 4 Whole leaf phosphorus (P) and calcium (Ca) concentrations. (a) Mean leaf P concentration for each species, with study area indicated by shading. (b) Total mean P concentration for Australian and South American (Brazil and Chile) Proteaceae species. (c) Mean leaf Ca concentration for each species, with study area indicated by shading. (d) Total mean Ca concentration for Australian and South American (Brazil and Chile) species. All concentrations are per unit dry weight and represent the entire leaf; therefore, values are not directly comparable with cell-specific concentrations, which are per unit fresh weight and represent individual cell types. Error bars show 95% confidence intervals from linear mixed-effect models. The different letters indicate significant differences (based on 95% confidence intervals) among species (a and c) or regions (b and d)
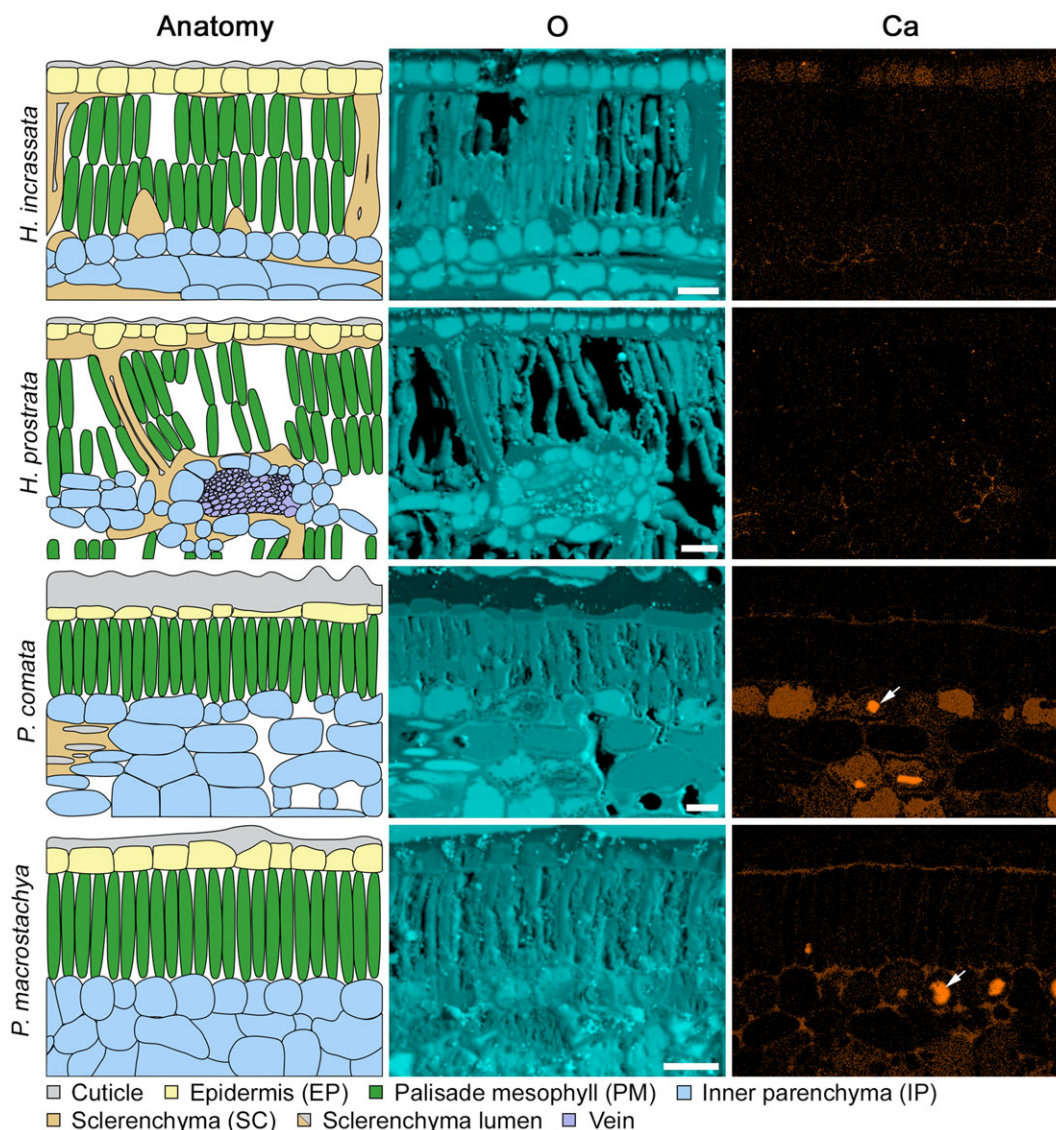
FIGURE 5 Qualitative element maps and corresponding anatomical schematics, showing calcium (Ca) and oxygen (O) distributions in transverse leaf sections of Australian species with isobilateral leaf anatomy (*Hakea incrassata*, *Hakea prostrata*, *Persoonia comata*, and *Petrophile macrostachya*). All leaves were isobilateral, with images capturing at least half of the transverse section. Calcium maps are corrected for peak overlaps and background subtraction and provide a visualization of the distribution, with quantified concentrations in Figures 2, 3. We did not present element maps for P, because they do not clearly show the distribution of P; however, P was accurately quantified from regions of interest (see Figure S1f–h). White arrows indicate Ca-based crystals. Scale bar: 50 μm

There was significant variation in patterns of Ca accumulation among species, including species of the same genus (Figure 6). For example, *B. menziesii* was the only *Banksia* species to accumulate Ca in HY (Figure 6), despite all *Banksia* species naturally co-occurring. Interestingly, Ca did not always accumulate in every cell of a particular cell type (Figures 5–7). For example, *P. comata* accumulated Ca in IP but not in all cells of the IP (Figure 5), whereas *L. ferruginea* accumulated Ca within PM and SM but also not in all of these cells (Figure 7).

At the species level, the greatest mean [Ca] was 1,413 μmol g^{-1} (PM.Ca, *L. ferruginea*, Chile) and the lowest was ~2 μmol g^{-1} (EP and PM, *E. coccineum*, Chile; Figure 3). The concentration of Ca within Ca-accumulating cell types of Australian species ranged from 127 μmol g^{-1} (IP.Ca, *P. macrostachya*) to 348 μmol g^{-1} (SM.Ca, *B. prionotes*; Figure 2). South American species showed a much larger range, from

97 μmol g^{-1} (SM.Ca, *L. hirsuta*) to 1,413 μmol g^{-1} (PM.Ca, *L. ferruginea*; Figure 3). Leaf Ca obviously not only varied in location but also in concentration. Calcium-based crystals were observed in six of the 12 species (white arrows, Figures 5–7). They ranged from ~2 to ~40 μm in size and tended to be formed within cells that accumulated Ca, such as SM.Ca in *Banksia* species (Figure 6). These crystals were avoided when analysing cellular regions so as not to misrepresent cellular Ca levels.

Despite the exceptionally high [Ca] reported in PM.Ca cells of *L. ferruginea* (~1,413 μmol g^{-1}), we are confident that this Ca was not mineralised, in either a crystalline or an amorphous form, based on optical imaging, electron microscopy, and 3-D X-ray microscopy (microCT). Across all of these techniques and analyses, we found no evidence of crystalline or amorphous material in these high-Ca cells of the PM (Figure S7). The Ca is contained within a large vacuole and
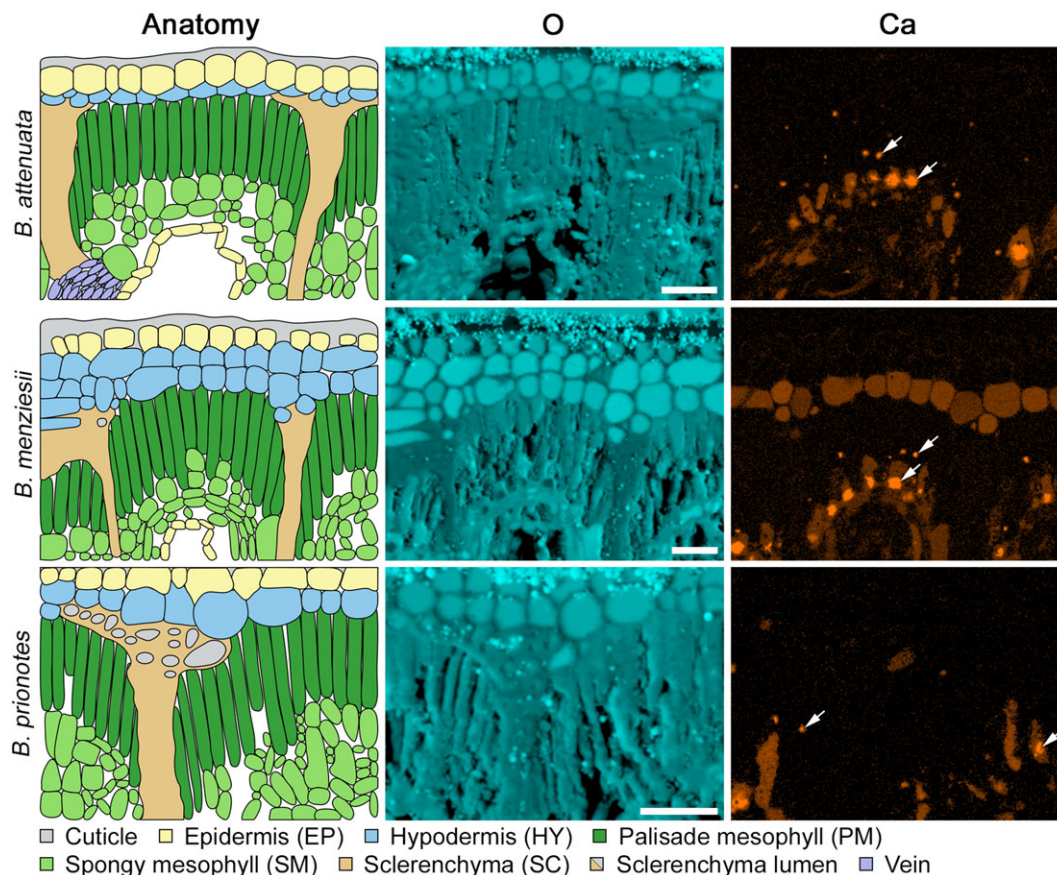
FIGURE 6 Qualitative element maps and corresponding anatomical schematics, showing calcium (Ca) and oxygen (O) distributions in transverse leaf sections of Australian species from the genus *Banksia* (*Banksia attenuata*, *Banksia menziesii*, and *Banksia prionotes*). All leaves were dorsiventral with stomatal crypts on the abaxial surface. Images capture upper part of transverse sections, with the adaxial surface at the top. Calcium maps are corrected for peak overlaps and background subtraction and provide a visualization of the distribution, with quantified concentrations in Figures 2, 3. We did not present element maps for P, because they do not clearly show the distribution of P; however, P was accurately quantified from regions of interest (see Figure S1f–h). White arrows indicate Ca-based crystals. Scale bar: 50 μm

is isolated from the cytoplasm (Figure S7a,b); it also has comparatively low water content and high [S] relative to the PM cells (60 ± 4 μmol S g^{-1} in PM.Ca vs. 11 ± 4 μmol S g^{-1} in PM; Figure S7c,d). Furthermore, the Ca within these cells is only ~5.7 atomic wt%, which is considerably lower than what we would expect if these were pure calcium oxalate minerals (31 atomic wt%) or plant-based calcium oxalate minerals (~22 atomic wt% in *B. attenuata* and *B. prionotes*, n = 12). Therefore, although the [Ca] is very high by cellular standards, it is actually very low by mineral standards. Consistent with this, 3-D X-ray microscopy scans revealed that the high-Ca cell layer in *Lomatia* is considerably less dense than that of typical Ca-based minerals present in leaves (Figure S7e,f).

On average, whole leaf [Ca] in Proteaceae species from south-western Australia (4.90 mg g^{-1} DW) were not significantly different to those from South America (6.39 mg g^{-1} DW; Brazil and Chile; Figure 4 and Table S4). Leaf [Ca] in Proteacea species from south-western Australia ranged from 2.6 mg g^{-1} DW in *H. prostrata* to 6.7 mg g^{-1} DW in *B. menziesii* (Figure 4 and Table S4). Whereas in South America, leaf [Ca] ranged from 2.60 mg g^{-1} DW in *E. coccineum* (Chile) to 12.47 mg g^{-1} DW in *L. ferruginea* (Chile; Figure 4 and Table S4).

4 | DISCUSSION

4.1 | Phosphorus

Phosphorus was preferentially allocated to photosynthetic cells in Proteaceae from extremely P-impoverished habitats in south-western Australia. However, this is clearly not a family-wide trait, as it was not found in species from P-richer soils in Brazil and Chile. We, therefore, show that P distribution patterns vary within a single eudicot family, contrary to the model that eudicots follow a single general pattern (Conn & Gilliham, 2010). The accumulation of P within photosynthetic cells contributes towards a high PPUE and may be linked to improved P-resorption in these species (Lambers, Finnegan, et al., 2015) and is thus likely an adaptation to severely P-impoverished habitats.

The current model for P distribution in eudicots is that they typically accumulate P in EP and BS cells and exclude it from mesophyll cells (PM and SM) (Conn & Gilliham, 2010). In contrast, Proteaceae from Australia showed a clear preferential allocation of P to these photosynthetic mesophyll cells, whereas species from South America showed much lower but consistent [P] across all cell types. Therefore,
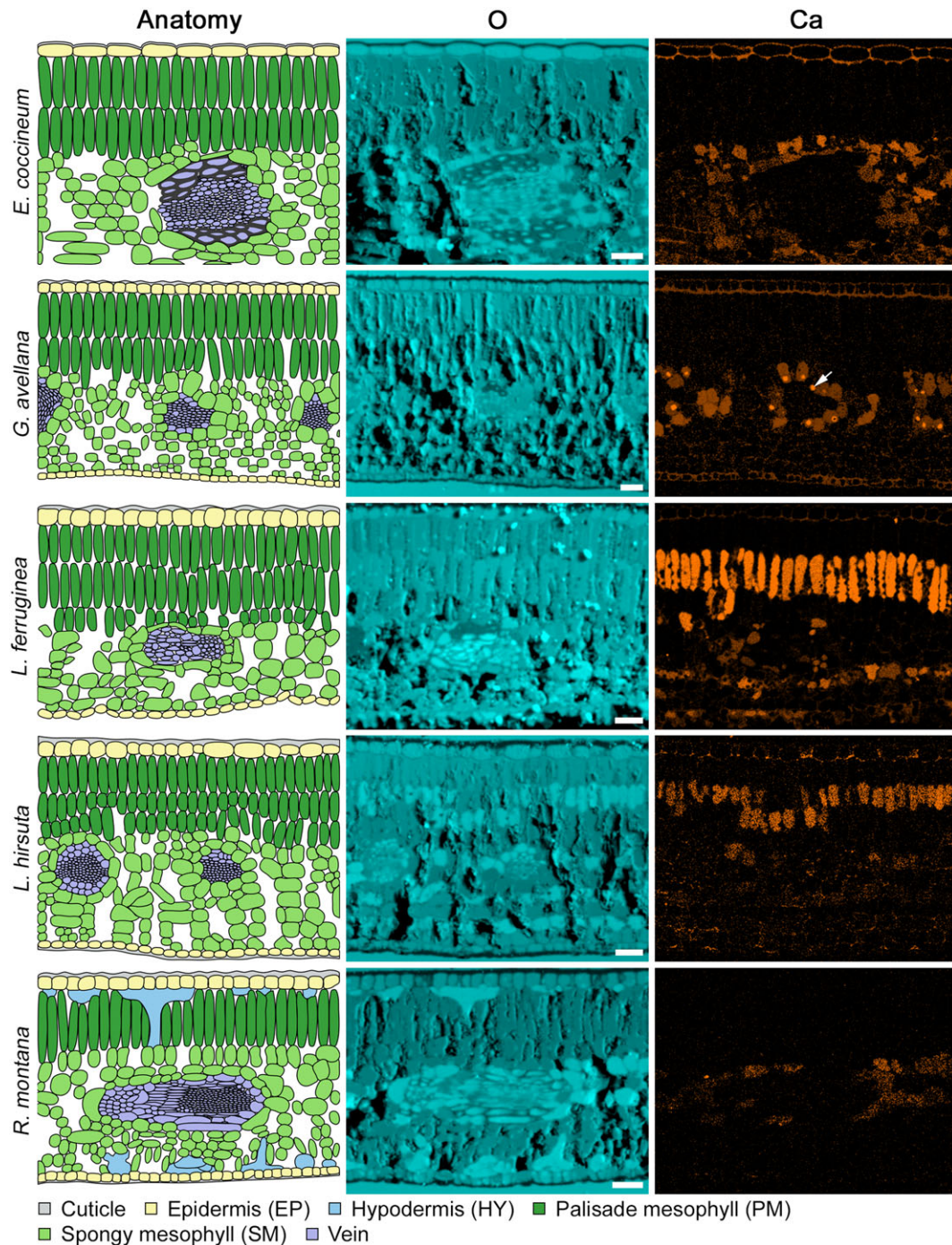
FIGURE 7 Qualitative element maps and corresponding anatomical schematics, showing calcium (Ca) and oxygen (O) distributions in transverse leaf sections of South American species (*Embothrium coccineum*, *Gevuina avellana*, *Lomatia ferruginea*, *Lomatia hirsuta*, and *Roupala montana*). All leaves were dorsiventral, with the adaxial surface at the top. All species were collected in Chile, except for *Roupala montana*, which was collected in Brazil. Calcium maps are corrected for peak overlaps and background subtraction and provide a visualization of the distribution, with quantified concentrations in Figures 2, 3. We did not present element maps for P, because they do not clearly show the distribution of P; however, P was accurately quantified from regions of interest (see Figure S1f–h). White arrows indicate Ca-based crystals. Scale bar: 50 μm

none of the 12 species studied followed the current model of P allocation (Conn & Gilliham, 2010). Furthermore, this trait appears to be under genetic control and is unlikely a phenotypic response to the environment; as the same preferential allocation of P is maintained under high P-supply in *H. prostrata* (Shane et al., 2004). Hence, patterns of P allocation vary within eudicots and even within a single family.

Preferential allocation of P to mesophyll cells has also been observed in *Leucadendron* "Safari Sunset," a Proteaceae from a severely P-impoverished habitat in South Africa (Hawkins et al., 2008), as well as in two species from severely P-impoverished south-western Australia (Lambers, Finnegan, et al., 2015; Shane et al., 2004). The consistent presence of this trait in Proteaceae from severely P-impoverished habitats and its absence in Proteaceae from other P-

richer habitats suggests that it has evolved as an adaptation to severely P-impoverished conditions. (Hawkins et al., 2008; Lambers, Finnegan, et al., 2015; Shane et al., 2004). Species from these severely P-impoverished habitats commonly show extremely high PPUE: 170 to 500 µmol CO_2 [g leaf P]$^{-1}$ s^{-1} (Proteaceae from south-western Australia, Denton et al., 2007; Lambers et al., 2012), compared with 100 µmol CO_2 [g leaf P]$^{-1}$ s^{-1} for species in a global comparison, including different families (Wright et al., 2004), and compared with Proteaceae species from P-richer habitats in South America, 90 to 140 µmol CO_2 [g leaf P]$^{-1}$ s^{-1} (Table S1; Franco, 1998; Wright et al., 2004; Franco et al., 2005). Such exceptionally high values of PPUE are achieved by maintaining rapid rates of photosynthesis at extremely low leaf [P] (Table S1). We surmise that by preferentially allocating P, these species are able to reduce their whole leaf [P], while maintaining high [P] in photosynthetic cells and thus still able to achieve rapid rates of photosynthesis (Stitt et al., 2010). Therefore, the ability of Proteaceae from severely P-impoverished habitats to preferentially allocate P to photosynthetic cells offers a partial explanation for their extremely high PPUE and may represent a critically important adaptation to surviving in a P-limited habitat. Other traits that contribute to a high PPUE are replacement of phospholipids by sulfolipids and galactolipids (Lambers et al., 2012) and functioning at very low levels of ribosomal RNA (Sulpice et al., 2014).

Proteaceae from severely P-limited south-western Australia show whole leaf [P] approximately half that of Proteaceae from P-richer parts of South America. Yet despite their extremely low whole leaf [P], the Australian Proteaceae are still able to maintain relatively rapid photosynthetic rates (10–22 µmol CO_2 m^{-2} s^{-1}; Denton et al., 2007; Lambers et al., 2012), even faster than species from South America (8.9–14 µmol CO_2 m^{-2} s^{-1}; Table S1; Franco, 1998; Wright et al., 2004; Franco et al., 2005). This can be partially explained by the ability of Australian Proteaceae to preferentially allocate P to photosynthetic cells and their ability to significantly reduce the [P] of non-photosynthetic cells. This results in Australian Proteaceae with photosynthetic cells that are ~6.5-fold greater in [P] than non-photosynthetic cells, reaching [P] that are up to ~2.5-fold greater than that of comparable photosynthetic cells in South American Proteaceae. However, these P-rich photosynthetic cells in the Australian Proteaceae only represent a small fraction of the whole leaf, with P-poor non-photosynthetic cells representing the larger proportion. Therefore, the exceptionally high [P] of photosynthetic cells in the Australian Proteaceae are effectively diluted by the extremely low [P] of the larger non-photosynthetic portion of the leaf. Therefore, although Proteaceae from south-western Australia have exceptionally low whole leaf [P], they are still able to maintain high [P] in their photosynthetic cells, and thus, they are able to achieve rapid rates of photosynthesis along with exceptionally high PPUE.

Outside of the Proteaceae, monocot species also preferentially allocate P to mesophyll cells (Conn & Gilliham, 2010). Interestingly, these monocot species also show high values of PPUE (Halsted & Lynch, 1996). With this, Proteaceae from P-impoverished habitats, as well as monocot species, both preferentially allocate P to photosynthetic mesophyll cells and show high PPUE. Therefore, there is a growing body of support highlighting a link between allocation of P to photosynthetic cells and a high P-use efficiency.

Increased capacity to resorb and reallocate P from senescing leaves is another trait common to Proteaceae from P-impoverished habitats; this trait improves overall plant P-use efficiency by decreasing the plants demand on external P. Proteaceae from P-impoverished south-western Australia are known to resorb up to ~90% of P from senescing leaves (Denton et al., 2007; Hayes et al., 2014; Wright et al., 2004), whereas Proteaceae from relatively P-richer habitats in South America show much lower levels of P-resorption efficiency, ~13% (*E. coccineum* and *L. hirsuta*; Diehl et al., 2003; Lambers et al., 2012). The ability to preferentially allocate P to mesophyll cells may allow for improved leaf P-resorption, because, by allocating P to a specific region, this can allow for a more localized and efficient expression of phosphatase enzymes, required to breakdown organic P to inorganic P, which can then be more efficiently exported from the leaf, due to the close proximity of mesophyll cells to the phloem, through which P is exported. Therefore, we hypothesize that there is a link between the preferential allocation of P to mesophyll cells and increased P-resorption.

Our results do not support the current model of cell-specific P allocation patterns in eudicot leaves; this discrepancy may be explained by the fact that most studies in this field have focused on metal-hyperaccumulating species and/or crop species (Ager, Ynsa, Domínguez-Solís, Gotor, et al., 2002; Ager, Ynsa, Domínguez-Solís, López-Martín, et al., 2003; Bidwell et al., 2004; Fernando et al., 2006; Fernando et al., 2008; Küpper, et al., 1999; Küpper, Lombi, Zhao, & McGrath, 2000; Küpper, Lombi, Zhao, Wieshammer, et al., 2001 ; Mesjasz-Prybylowicz & Pineda, 2001; Mesjasz-Przybylowicz et al., 2001; Mesjasz-Przybyłowicz et al., 1994; Regvar et al., 2013; Rios et al., 2012; Treeby et al., 1987; Villafort Carvalho et al., 2015; Vogel-Mikuš et al., 2008, 2014; Zhao et al., 2000). These species likely function very differently in their environment, compared with native species from nutrient-poor habitats. Therefore, our results are significant in broadening this field of research and adding to a more comprehensive understanding of P use in eudicots.

There is a clear need for more research into cell-type-specific P distribution patterns across a more phylogenetically and ecologically diverse range of species. This will enhance our understanding of the factors underlying P distribution within plants, with significant implications for plant physiology, species distribution, and community functioning. By further investigation and improved understandings of the subcellular processes and mechanisms involved in P allocation and their link to improving whole-plant P-use efficiency, we will be able to improve crop breeding efforts, with the aim of decreasing society's demand for P in food production (Veneklaas et al., 2012).

4.2 | Calcium

Calcium distribution patterns varied among species and, therefore, also did not reflect the notion of a single pattern in all eudicots (Conn & Gilliham, 2010). All species accumulated Ca within specific cell types, but these cell types differed among species, with no clear shift between species that did or did not allocate P to mesophyll cells. Calcium-accumulating cells were not always along the transpiration pathway and were generally separate from P-accumulating cells. Calcium typically accumulated within IP and SM, but, importantly, many species

also accumulated Ca within other cell types/regions. Variation in Ca accumulation strategies was even observed within a single genus, in co-occurring *Banksia* species.

The mechanisms underlying cell-specific accumulation of Ca and other elements are not fully understood (Conn et al., 2011; Conn & Gilliham, 2010; Gilliham et al., 2011; White & Broadley, 2003). Calcium primarily moves through leaves via the transpirational movement of water, from xylem to stomata (White, 2001; White & Broadley, 2003). Consequently, Ca is thought to accumulate primarily in cells along this path, such as SM, due to their greater apoplastic [Ca] ($[Ca^{2+}]_{apo}$; Gilliham et al., 2011; Karley, Leigh, & Sanders, 2000). The accumulation of Ca within SM (in *G. avellana* and *R. montana*) supports this model, as these areas are close to the xylem and typically show greater $[Ca^{2+}]_{apo}$ (Gilliham et al., 2011; Kerton, Newbury, Hand, & Pritchard, 2009; White, 2001). However, for cells to accumulate Ca within their vacuole, they must also express both Ca^{2+}-permeable ion channels, allowing Ca^{2+} to move down an electrochemical potential gradient into the cytosol, and tonoplast-localized transporters, allowing Ca^{2+} uptake against an electrochemical potential gradient (Ca^{2+}-transporting P-type-ATPases and Ca^{2+}/H^+ antiporters), into the vacuole, where it can accumulate to high concentrations (>1,400 μmol g^{-1}; Conn et al., 2011; Mäser et al., 2001; McAinsh & Pittman, 2009; Shigaki & Hirschi, 2006).

We found that Ca accumulated in PM of *Lomatia* species and HY of *B. menziesii*. In these species, Ca accumulated in specific and distinct layers of cells, not located along the transpiration pathway, that is, not between the xylem and stomata. We, therefore, suggest that in these species, the transpiration pathway is not the major determinant of leaf cell-specific Ca accumulation; instead, it is likely primarily driven by the differential expression of Ca^{2+} channels/transporters that function to accumulate Ca within vacuoles of specific cells, thus functioning to maintain $[Ca^{2+}]_{apo}$ and cytosolic $[Ca^{2+}]$ ($[Ca^{2+}]_{cyt}$). This has also been demonstrated in *Arabidopsis*, where the preferential expression of a tonoplast Ca^{2+}/H^+ antiporter *CAX1* in mesophyll cells is necessary for the preferential storage of Ca in these cells (Conn et al., 2011). In summary, the movement of water via transpiration is vital for the overall uptake and regulation of Ca in leaves (McLaughlin & Wimmer, 1999), but, on the basis of the patterns of Ca distribution, this is not invariably the primary mechanism underlying cell-specific accumulation of Ca in leaves. We suggest that the ability of specific cells to accumulate large amounts of Ca is primarily driven by a higher expression of Ca^{2+}-channels and tonoplast Ca^{2+} transporters and is less reliant on the movement of water through leaves. This uncoupling of Ca^{2+} accumulation from water flow has also been demonstrated in other studies (Atkinson, Ruiz, & Mansfield, 1992; Kerton et al., 2009; Storey & Leigh, 2004). There is a need for further research into the differential expression of these channels and transporters within contrasting cell types, particularly in species such as *Lomatia*, where Ca accumulates preferentially in distinct layers of what appears to be the one cell type.

Exceptionally high [Ca] of ~1,413 μmol g^{-1} was observed in PM.Ca cells of *L. ferruginea*. At this concentration, it is highly unlikely that the Ca is in a readily soluble or ionic (Ca^{2+}) form, due to the necessary cellular counterbalancing that would be required to maintain this level of Ca within the cell vacuole. However, as evidenced by a range of techniques, we are certain that this Ca is not mineralised, either in a crystalline or an amorphous form. On the basis of the evidence, we surmise that the Ca is bound to Ca-binding proteins within the vacuole (supported by higher [S]), allowing for such high concentrations to be accumulated and stabilized. Further investigation of this unique phenomenon may yield exciting details regarding Ca regulation and accumulation in higher plants.

As hypothesized, almost all species allocated P and Ca to different cell types, thus avoiding precipitation of calcium phosphate. The only exception to this were the Australian *Banksia* species, which preferentially allocated both Ca and P to SM cells. Despite preferential allocation, [P] in these Ca-accumulating cells remained very low, at <10 μmol g^{-1}. Maintenance of a low [P] may partly explain an ability to co-allocate these elements. The physiological implications of such P/Ca co-allocation are not yet known but might be relevant in understanding symptoms of P-toxicity, which are known to increase under higher Ca availability for many Proteaceae (Grundon, 1972).

4.3 | Concluding remarks

Our study shows that leaf cell-type-specific distribution of P and Ca varies significantly among Proteaceae. This finding is in contrast with the current model and highlights the need for a better understanding of the underlying roles and mechanisms of cell-specific element accumulation within plants. The accumulation of P in photosynthetic cells of species from low-P habitats partially explains their very high PPUE. Further research is needed to determine if this pattern is found in other species, outside the Proteaceae, that are also adapted to severely P-impoverished habitats. The link between accumulating P in photosynthetic cells and a high PPUE is highly applicable in improving P-use efficiency for crop species and thus reducing the P-demand of food production worldwide.

The extent to which cell-specific element accumulation varies among a range of ecologically and phylogenetically diverse species remains to be further investigated, as do the mechanisms underlying it. This knowledge will improve our understanding of the movement, accumulation, and overall regulation of essential elements within plants. An improved understanding of these processes will greatly benefit applied fields of research, such as the bio-fortification of our staple foods (Dayod, Tyerman, Leigh, & Gilliham, 2010; Pinto & Ferreira, 2015; Rios et al., 2012), phytoremediation/phytoextraction of contaminated soils (Shigaki & Hirschi, 2006), and improved nutrient-use efficiency in crop plants (Lambers, Clode, et al., 2015; Veneklaas et al., 2012).

AUTHOR CONTRIBUTION

ORCID

Patrick E. Hayes http://orcid.org/0000-0001-7554-4588

REFERENCES

Ager, F. J., Ynsa, M. D., & Domínguez-Solís J.R., Gotor C., Respaldiza M.A. & Romero L.C. (2002). Cadmium localization and quantification in the plant *Arabidopsis thaliana* using micro-PIXE. *Nuclear Instruments and Methods in Physics Research Section B: Beam Interactions with Materials and Atoms*, 189, 494–498.

Ager, F. J., Ynsa, M. D., & Domínguez-Solís J.R., López-Martín M.C., Gotor C. & Romero L.C. (2003). Nuclear micro-probe analysis of *Arabidopsis thaliana* leaves. *Nuclear Instruments and Methods in Physics Research Section B: Beam Interactions with Materials and Atoms*, 210, 401–406.

Atkinson, C. J., Ruiz, L. P., & Mansfield, T. A. (1992). Calcium in xylem sap and the regulation of its delivery to the shoot. *Journal of Experimental Botany*, 43, 1315–1324.

Bidwell, S. D., Crawford, S. A., Woodrow, I. E., Sommer-Knudsen, J., & Marshall, A. T. (2004). Sub-cellular localization of Ni in the hyperaccumulator, Hybanthus floribundus (Lindley) F. Muell. *Plant, Cell & Environment*, 27, 705–716.

Borie, F., & Rubio, R. (2003). Total and organic phosphorus in Chilean volcanic soils. *Gayana. Botánica*, 60, 69–73.

Carter, M. R., & Gregorich, E. G. (Eds.) (2008). *Soil sampling and methods of analysis* (2nd ed.). Boca Raton, FL: Canadian Society of Soil Science; CRC press.

Conn, S., & Gilliham, M. (2010). Comparative physiology of elemental distributions in plants. *Annals of Botany*, 105, 1081–1102.

Conn, S. J., Gilliham, M., Athman, A., Schreiber, A. W., Baumann, U., Moller, I., ... Leigh, R. A. (2011). Cell-specific vacuolar calcium storage mediated by *CAX1* regulates apoplastic calcium concentration, gas exchange, and plant productivity in *Arabidopsis*. *Plant Cell*, 23, 240–257.

Core Team, R. (2016). *R: A language and environment for statistical computing*. Vienna, Austria: R Foundation for Statistical Computing.

Cowling, R. M., & Lamont, B. B. (1998). On the nature of Gondwanan species flocks: Diversity of Proteaceae in Mediterranean south-western Australia and South Africa. *Australian Journal of Botany*, 46, 335–355.

Dayod, M., Tyerman, S. D., Leigh, R. A., & Gilliham, M. (2010). Calcium storage in plants and the implications for calcium biofortification. *Protoplasma*, 247, 215–231.

Delgado, M., Zúñiga-Feest, A., Almonacid, L., Lambers, H., & Borie, F. (2015). Cluster roots of *Embothrium coccineum* (Proteaceae) affect enzyme activities and phosphorus lability in rhizosphere soil. *Plant and Soil*.

Denton, M. D., Veneklaas, E. J., Freimoser, F. M., & Lambers, H. (2007). *Banksia* species (Proteaceae) from severely phosphorus-impoverished

soils exhibit extreme efficiency in the use and re-mobilization of phosphorus. *Plant, Cell and Environment*, 30, 1557–1565.

Diehl, P., Mazzarino, M. J., Funes, F., Fontenla, S., Gobbi, M., & Ferrari, J. (2003). Nutrient conservation strategies in native Andean-Patagonian forests. *Journal of Vegetation Science*, 14, 63–70.

Fernando, D. R., Bakkaus, E. J., Perrier, N., Baker, A. J. M., Woodrow, I. E., Batianoff, G. N., & Collins, R. N. (2006). Manganese accumulation in the leaf mesophyll of four tree species: A PIXE/EDAX localization study. *The New Phytologist*, 171, 751–757.

Fernando, D. R., Woodrow, I. E., Jaffré, T., Dumontet, V., Marshall, A. T., & Baker, A. J. M. (2008). Foliar manganese accumulation by Maytenus founieri (Celastraceae) in its native New Caledonian habitats: Populational variation and localization by X-ray microanalysis. *New Phytologist*, 177, 178–185.

Fox, J. (2003). Effect displays in R for generalised linear models. *Journal of Statistical Software*, 8, 1–27.

Franco, A. C. (1998). Seasonal patterns of gas exchange, water relations and growth of it *Roupala montana*, an evergreen savanna species. *Plant Ecology*, 136, 69–76.

Franco, A. C., Bustamante, M., Caldas, L. S., Goldstein, G., Meinzer, F. C., Kozovits, A. R., ... Coradin, V. T. R. (2005). Leaf functional traits of Neotropical savanna trees in relation to seasonal water deficit. *Trees*, 19, 326–335.

Gilliham, M., Dayod, M., Hocking, B. J., Xu, B., Conn, S. J., Kaiser, B. N., ... Tyerman, S. D. (2011). Calcium delivery and storage in plant leaves: Exploring the link with water flow. *Journal of Experimental Botany*, 62, 2233–2250.

Grundon, N. J. (1972). Mineral nutrition of some Queensland heath plants. *Journal of Ecology*, 60, 171–181.

Halsted, M., & Lynch, J. (1996). Phosphorus responses of C3 and C4 species. *Journal of Experimental Botany*, 47, 497–505.

Hawkins, H.-J., Hettasch, H., Mesjasz-Przybylowicz, J., Przybylowicz, W., & Cramer, M. D. (2008). Phosphorus toxicity in the Proteaceae: A problem in post-agricultural lands. *Scientia Horticulturae*, 117, 357–365.

Hayes, P., Turner, B. L., Lambers, H., & Laliberté, E. (2014). Foliar nutrient concentrations and resorption efficiency in plants of contrasting nutrient-acquisition strategies along a 2-million-year dune chronosequence. *Journal of Ecology*, 102, 396–410.

Huang, C. X., Canny, M. J., Oates, K., & McCully, M. E. (1994). Planing frozen hydrated plant specimens for SEM observation and EDX microanalysis. *Microscopy Research and Technique*, 28, 67–74.

Jin, Q., Paunesku, T., Lai, B., Gleber, S.-C., Chen, S., Finney, L., ... Jacobsen, C. (2017). Preserving elemental content in adherent mammalian cells for analysis by synchrotron-based X-ray fluorescence microscopy. *Journal of Microscopy*, 265, 81–93.

Karley, A. J., Leigh, R. A., & Sanders, D. (2000). Where do all the ions go? The cellular basis of differential ion accumulation in leaf cells. *Trends in Plant Science*, 5, 465–470.

Kerton, M., Newbury, H. J., Hand, D., & Pritchard, J. (2009). Accumulation of calcium in the centre of leaves of coriander (*Coriandrum sativum* L.) is due to an uncoupling of water and ion transport. *Journal of Experimental Botany*, 60, 227–235.

Küpper, H., Lombi, E., Zhao, F. J., & McGrath, S. P. (2000). Cellular compartmentation of cadmium and zinc in relation to other elements in the hyperaccumulator *Arabidopsis halleri*. *Planta*, 212, 75–84.

Küpper, H., Lombi, E., Zhao, F. J., Wieshammer, G., & McGrath, S. P. (2001). Cellular compartmentation of nickel in the hyperaccumulators *Alyssum lesbiacum*, *Alyssum bertolonii* and *Thlaspi goesingense*. *Journal of Experimental Botany*, 52, 2291–2300.

Küpper, H., Zhao, F. J., & McGrath, S. P. (1999). Cellular compartmentation of zinc in leaves of the hyperaccumulator *Thlaspi caerulescens*. *Plant Physiology*, 119, 305.

Lambers, H., Bishop, J. G., Hopper, S. D., Laliberté, E., & Zúñiga-Feest, A. (2012). Phosphorus-mobilization ecosystem engineering: The roles of

cluster roots and carboxylate exudation in young P-limited ecosystems. *Annals of Botany*, *110*, 329–348.

Lambers, H., Brundrett, M. C., Raven, J. A., & Hopper, S. D. (2010). Plant mineral nutrition in ancient landscapes: High plant species diversity on infertile soils is linked to functional diversity for nutritional strategies. *Plant and Soil*, *334*, 11–31.

Lambers, H., Cawthray, G. R., Giavalisco, P., Kuo, J., Laliberté, E., Pearse, S. J., ... Turner, B. L. (2012). Proteaceae from severely phosphorus-impoverished soils extensively replace phospholipids with galactolipids and sulfolipids during leaf development to achieve a high photosynthetic phosphorus-use-efficiency. *New Phytologist*, *196*, 1098–1108.

Lambers, H., Clode, P. L., Hawkins, H.-J., Laliberté, E., Oliveira, R. S., Reddell, P., ... Weston, P. (2015). Metabolic adaptations of the non-mycotrophic Proteaceae to soils with low phosphorus availability. In W. C. Plaxton, & H. Lambers (Eds.), *Annual plant reviews volume 48* (pp. 289–335). John Wiley & Sons, Inc.

Lambers, H., Finnegan, P. M., Jost, R., Plaxton, W. C., Shane, M. W., & Stitt, M. (2015). Phosphorus nutrition in Proteaceae and beyond. *Nature Plants*, *1*, 15109.

Lannes, L., Bustamante, M., Edwards, P., & Olde, V. H. (2016). Native and alien herbaceous plants in the Brazilian Cerrado are (co-)limited by different nutrients. *Plant & Soil*, *400*, 231–243.

Marshall, A. T. (1982). X-ray depth distribution (φ (ϱz)) curves for X-ray microanalysis of frozen-hydrated bulk biological samples. *Micron*, *13*, 317–318.

Marshall, A. T. (2017). Quantitative x-ray microanalysis of model biological samples in the SEM using remote standards and the XPP analytical model. *Journal of Microscopy*, *00*, 1–8.

Marshall, A. T., & Clode, P. L. (2009). X-ray microanalysis of Rb+ entry into cricket Malpighian tubule cells via putative K^+ channels. *Journal of Experimental Biology*, *212*, 2977–2982.

Marshall, A. T., Goodyear, M. J., & Crewther, S. G. (2012). Sequential quantitative X-ray elemental imaging of frozen-hydrated and freeze-dried biological bulk samples in the SEM. *Journal of Microscopy*, *245*, 17–25.

Marshall, A. T., & Xu, W. (1998). Quantitative elemental X-ray imaging of frozen-hydrated biological samples. *Journal of Microscopy*, *190*, 305–316.

Mäser, P., Thomine, S., Schroeder, J. I., Ward, J. M., Hirschi, K., Sze, H., ... Guerinot, M. L. (2001). Phylogenetic relationships within cation transporter families of *Arabidopsis*. *Plant Physiology*, *126*, 1646–1667.

McAinsh, M. R., & Pittman, J. K. (2009). Shaping the calcium signature. *New Phytologist*, *181*, 275–294.

McCully, M. E., Canny, M. J., Huang, C. X., Miller, C., & Brink, F. (2010). Cryo-scanning electron microscopy (CSEM) in the advancement of functional plant biology: Energy dispersive X-ray microanalysis (CEDX) applications. *Functional Plant Biology*, *37*, 1011–1040.

McLaughlin, S. B., & Wimmer, R. (1999). Calcium physiology and terrestrial ecosystem processes. *New Phytologist*, *142*, 373–417.

Mesjasz-Prybylowicz, J., & Pineda, C. A. (2001). Nuclear microprobe studies of elemental distribution in apical leaves of the Ni hyperaccumulator Berkheya coddii. *South African Journal of Science*, *97*, 591.

Mesjasz-Przybyłowicz, J., Balkwill, K., Przybyłowicz, W. J., & Annegarn, H. J. (1994). Proton microprobe and X-ray fluorescence investigations of nickel distribution in serpentine flora from South Africa. *Nuclear Instruments and Methods in Physics Research Section B: Beam Interactions with Materials and Atoms*, *89*, 208–212.

Mesjasz-Przybylowicz, J., Przybylowicz, W. J., Rama, D. B. K., & Pineda, C. A. (2001). Elemental distribution in *Senecio anomalochrous*, a Ni hyperaccumulator from South Africa. *South African Journal of Science*, *97*, 593.

Miatto, R. C., Wright, I. J., & Batalha, M. A. (2016). Relationships between soil nutrient status and nutrient-related leaf traits in Brazilian cerrado and seasonal forest communities. *Plant and Soil*, *404*, 13–33.

Motomizu, S., Wakimoto, T., & Toei, K. (1983). Spectrophotometric determination of phosphate in river water with molybdate and malachite green. *Analyst*, *108*, 361–367.

Pate, J. S., Verboom, W. H., & Galloway, P. D. (2001). Co-occurrence of Proteaceae, laterite and related oligotrophic soils: Coincidental associations or causative inter-relationships? *Australian Journal of Botany*, *49*, 529–560.

Pinheiro, J., Bates, D., DebRoy, S., Sarkar, D., & Core Team, R. (2016). nlme: Linear and nonlinear mixed effects models. *R package version*, *3*, 1–128.

Pinheiro, J. C., & Bates, D. M. (2000). *Mixed-effects models in S and S-PLUS*. New York, USA: Springer.

Pinto, E., & Ferreira, I. M. P. L. V. O. (2015). Cation transporters/channels in plants: Tools for nutrient biofortification. *Journal of Plant Physiology*, *179*, 64–82.

Regvar, M., Eichert, D., Kaulich, B., Gianoncelli, A., Pongrac, P., & Vogel-Mikuš, K. (2013). Biochemical characterization of cell types within leaves of metal-hyperaccumulating *Noccaea praecox* (Brassicaceae). *Plant & Soil*, *373*, 157–171.

Rios, J. J., Lochlainn, S. Ó., Devonshire, J., Graham, N. S., Hammond, J. P., King, G. J., ... Broadley, M. R. (2012). Distribution of calcium (Ca) and magnesium (Mg) in the leaves of *Brassica rapa* under varying exogenous Ca and Mg supply. *Annals of Botany*, *109*, 1081–1089.

Roomans, G. M., & Dragomir, A. (2007). X-ray microanalysis in the scanning electron microscope. *Electron Microscopy: Methods and Protocols*, 507–528.

Sauquet, H., Weston, P. H., Anderson, C. L., Barker, N. P., Cantrill, D. J., Mast, A. R., & Savolainen, V. (2009). Contrasted patterns of hyperdiversification in Mediterranean hotspots. *Proceedings of the National Academy of Sciences*, *106*, 221–225.

Shane, M. W., McCully, M. E., & Lambers, H. (2004). Tissue and cellular phosphorus storage during development of phosphorus toxicity in *Hakea prostrata* (Proteaceae). *Journal of Experimental Botany*, *55*, 1033–1044.

Shigaki, T., & Hirschi, K. D. (2006). Diverse functions and molecular properties emerging for *CAX* cation/H+ exchangers in plants. *Plant Biology*, *8*, 419–429.

Stitt, M., Lunn, J., & Usadel, B. (2010). *Arabidopsis* and primary photosynthetic metabolism – More than the icing on the cake. *Plant Journal*, *61*, 1067–1091.

Storey, R., & Leigh, R. A. (2004). Processes modulating calcium distribution in citrus leaves. An investigation using X-ray microanalysis with strontium as a tracer. *Plant Physiology*, *136*, 3838–3848.

Sulpice, R., Ishihara, H., Schlereth, A., Cawthray, G. R., Encke, B., Giavalisco, P., ... Lambers, H. (2014). Low levels of ribosomal RNA partly account for the very high photosynthetic phosphorus-use efficiency of Proteaceae species. *Plant, Cell & Environment*, *37*, 1276–1298.

Treeby, M. T., van Steveninck, R. F. M., & de Vries, H. M. (1987). Quantitative estimates of phosphorus concentrations within *Lupinus luteus* leaflets by means of electron probe X-ray microanalysis. *Plant Physiology*, *85*, 331–334.

Tsujii, Y., Oikawa, M., & Kitayama, K. (2017). Significance of the localization of phosphorus among tissues on a cross-section of leaf lamina of Bornean tree species for phosphorus-use efficiency. *Journal of Tropical Ecology*, *33*, 237–240.

Turner, B. L., Hayes, P. E., & Laliberté, E. (2017). A climosequence of chronosequences in southwestern Australia. *bioRxiv*, 113308.

Turner, B. L., & Laliberté, E. (2015). Soil development and nutrient availability along a 2 million-year coastal dune chronosequence under species-rich mediterranean shrubland in southwestern Australia. *Ecosystems*, *18*, 287–309.

Veneklaas, E. J., Lambers, H., Bragg, J., Finnegan, P. M., Lovelock, C. E., Plaxton, W. C., ... Raven, J. A. (2012). Opportunities for improving phosphorus-use efficiency in crop plants. *New Phytologist*, *195*, 306–320.

Villafort Carvalho, M. T., Pongrac, P., Mumm, R., van Arkel, J., van Aelst, A., Jeromel, L., ... Aarts, M. G. M. (2015). *Gomphrena claussenii*, a novel

metal-hypertolerant bioindicator species, sequesters cadmium, but not zinc, in vacuolar oxalate crystals. *New Phytologist, 208*, 763–775.

Vogel-Mikuš, K., Pongrac, P., & Pelicon, P. (2014). Micro-PIXE elemental mapping for ionome studies of crop plants. *International Journal of PIXE, 24*, 217–233.

Vogel-Mikuš, K., Simčič, J., Pelicon, P., Budnar, M., Kump, P., Nečemer, M., ... Regvar, M. (2008). Comparison of essential and non-essential element distribution in leaves of the Cd/Zn hyperaccumulator *Thlaspi praecox* as revealed by micro-PIXE. *Plant, Cell & Environment, 31*, 1484–1496.

Weston, P., & Barker, N. (2006). A new suprageneric classification of the Proteaceae, with an annotated checklist of genera. *Telopea*, 314–344.

Weston, P. H. (2007). Proteaceae. In *Flowering plants eudicots* (pp. 364–404). Berlin-Heidelberg: Springer-Verlag.

Weston, P. H. (2014). What has molecular systematics contributed to our knowledge of the plant family Proteaceae? In P. Besse (Ed.), *Molecular plant taxonomy* (pp. 365–397). Totowa, NJ: Humana Press.

White, P. J. (2001). The pathways of calcium movement to the xylem. *Journal of Experimental Botany, 52*, 891–899.

White, P. J., & Broadley, M. R. (2003). Calcium in plants. *Annals of Botany, 92*, 487–511.

Wright, I. J., Reich, P. B., Westoby, M., Ackerly, D. D., Baruch, Z., Bongers, F., ... Villar, R. (2004). The worldwide leaf economics spectrum. *Nature, 428*, 821–827.

Zhao, F. J., Lombi, E., Breedon, T., & McGrath, S. P. (2000). Zinc hyperaccumulation and cellular distribution in *Arabidopsis halleri*. *Plant, Cell & Environment, 23*, 507–514.

SUPPORTING INFORMATION

Additional Supporting Information may be found online in the supporting information tab for this article.